

Catalysis Science & Technology

Accepted Manuscript



This is an *Accepted Manuscript*, which has been through the Royal Society of Chemistry peer review process and has been accepted for publication.

Accepted Manuscripts are published online shortly after acceptance, before technical editing, formatting and proof reading. Using this free service, authors can make their results available to the community, in citable form, before we publish the edited article. We will replace this *Accepted Manuscript* with the edited and formatted *Advance Article* as soon as it is available.

You can find more information about *Accepted Manuscripts* in the [Information for Authors](#).

Please note that technical editing may introduce minor changes to the text and/or graphics, which may alter content. The journal's standard [Terms & Conditions](#) and the [Ethical guidelines](#) still apply. In no event shall the Royal Society of Chemistry be held responsible for any errors or omissions in this *Accepted Manuscript* or any consequences arising from the use of any information it contains.



Catalysis Science & Technology

ARTICLE

A self-emulsifying catalytic system for the aqueous biphasic hydroformylation of triglycerides

Received 00th January 20xx,
Accepted 00th January 20xx

T. Vanbésien,^{a,b} A. Sayede,^{a,b} E. Monflier^{a,b} and F. Hapiot^{*a,b}

DOI: 10.1039/x0xx00000x

The Rh-catalyzed hydroformylation of the C=C double bonds of triglycerides (**T**) was performed in aqueous medium through the formation of supramolecular complexes resulting from the inclusion of alkenyl chains of **T** into the cavity of modified cyclodextrins (CDs). Mixing **T** and the aqueous catalytic phase in the presence of CDs led to emulsions that were characterized by phase diagrams and nephelometric measurements. Variations of the nature of the CDs, the reaction temperature, the CO/H₂ pressure and the nature of the catalyst allowed for the optimization of the catalytic conditions. The concept was efficiently applied to commercial oils. Molecular dynamics simulations corroborated experimental data.

www.rsc.org/

Introduction

In recent years, the increasing number of articles related to the functionalization of triglycerides reflects the growing interest of researchers in the field. The main advantage of triglycerides over other bio-sourced molecules lies in the richness of their chemical structure. The ester functions can be easily hydrolyzed to provide a wide range of fatty acids methyl esters (FAMES). Moreover, the C=C double bonds of the long alkyl chains can be functionalized or cleaved to yield countless bio-sourced products. The C=C double bond could undergo oxidation, epoxidation, metathesis or hydroformylation reactions, to name only some of the possible transformation.^{1,2,3} Triglycerides hydroformylation is of particular interest from an industrial viewpoint as the resulting aldehydes can be easily converted into alcohol, acids or amines, three functional groups classically encountered in polymer chemistry. The first studies about triglycerides hydroformylation date back from the 60's with the works of Lai, Naudet and Ucciani.^{4,5} Their pioneering works were then followed in the 70's by a systematic study through which Frankel et al. demonstrated the viability of the triglycerides hydroformylation on an industrial scale.⁶ In the 90's, Fell et al. demonstrated that surfactants could be used as mass transfer promoters in hydroformylation of FAME.⁷ Van Leeuwen and coworkers proceeded to a series of hydroformylation experiments with a high-grade and a technical-grade derived methyl oleate (MO) and a Rh-catalyst coordinated by bulky phosphites.⁸ Mild conditions were used to hydroformylate high-grade MO while harsher

conditions were required for technical-grade derived MO because of the presence in the mixture of methyl linoleate, which inactivated the Rh-catalyst by μ -allyl coordination. Intricate mixtures of products were obtained in that case. Kandamarachchi et al. showed that triphenylphosphine yielded a higher reactivity than triphenylphosphite in Rh-hydroformylation of vegetable oils (soybean, high oleic safflower, safflower, and linseed) and model compounds (methyl linoleate, methyl oleate, **T**, and trilinolein).^{9,10} da Rosa and coworkers performed Rh-catalyzed hydroformylation of ethyl ricinoleate and castor oil under mild conditions to achieve complete conversion of double bonds within 6 h.¹¹ Only small amounts of aldehydes could be identified as an intramolecular condensation between carbonyl and hydroxyl groups preferentially led to 2-hydroxy-furans. The hydroformylation of technical-grade MO and soybean oil was also reported by the same authors.¹² HRh(CO)(PPh₃)₃ proved to be much more effective as catalyst precursor than RhCl₃·3H₂O to access aldehydes. Later, they described the Rh-catalyzed hydroformylation of methyl oleate using PEGPHOT (tri-(4-triethylenoglycolmonomethyletherphenyl) phosphite) as ligand in a biphasic system consisting of PEG-400 and methyl oleate.¹³ However, 50% undesired hydrogenated compounds were produced along with 50% aldehydes. Ionic liquids were also used to stabilize a Rh-complex in its active form for the hydroformylation of soybean biodiesel (24% alkyl oleate, 54% linoleate and 6% linolenate).¹⁴ Quantitative yields of aldehydes were obtained within 8 h. However, the rhodium leaching to the organic phase prevented an effective catalyst recovery. Using the chelating biphosphite ligand BIPHEPHOS, Behr et al. demonstrated that MO and ethyl linoleate could undergo an isomerizing hydroformylation at 115 °C under 20 bar CO/H₂ leading to linear aldehydes.¹⁵ However, the yields remained modest (26 and 34%, respectively) due to a very strong hydrogenation side reaction. Lactame-based phosphoramidite ligands of different size (four- to seven-membered rings) also proved to be effective in the Rh-catalyzed hydroformylation of methyl oleate.¹⁶ The latter was also subjected to the tandem

^a Univ. Artois, UMR 8181, Unité de Catalyse et de Chimie du Solide (UCCS), F-62300 Lens, France. E-mail: frederic.hapiot@univ-artois.fr

^b CNRS, UMR 8181, Unité de Catalyse et de Chimie du Solide (UCCS), Lille, F-59000, France.

Electronic Supplementary Information (ESI) available: Formation of CD/T supramolecular complexes, Gibbs equations, interfacial excess, interfacial area and CD/T stoichiometry, catalytic experiments, ¹H NMR spectra of reactant and product, conversion calculations, catalytic results, nephelometric measurements and Stokes equations. See DOI: 10.1039/x0xx00000x

isomerization/hydroformylation/hydrogenation reaction using a combination of Rh(acac)(CO)₂, Shvo's catalyst and phosphorus ligands.¹⁷ The expected *n*-alcohol was formed (37%) along with large amounts of hydrogenated products (29%). Very recently, the hydroformylation of internal C=C double bonds was developed using either conventional heating or microwave irradiation (MW).¹⁸ Methyl oleate was efficiently converted (up to 98% conv.) with high chemoselectivities (up to 98%) using a combination of bulky aryl monophosphites ligands and Rh-catalyst. Very recently, the isomerizing hydroformylation of the internal carbon-carbon double bond of methyl oleate was performed with high regioselectivity (75% linear isomer) using a bis(phosphite) ligand.¹⁹

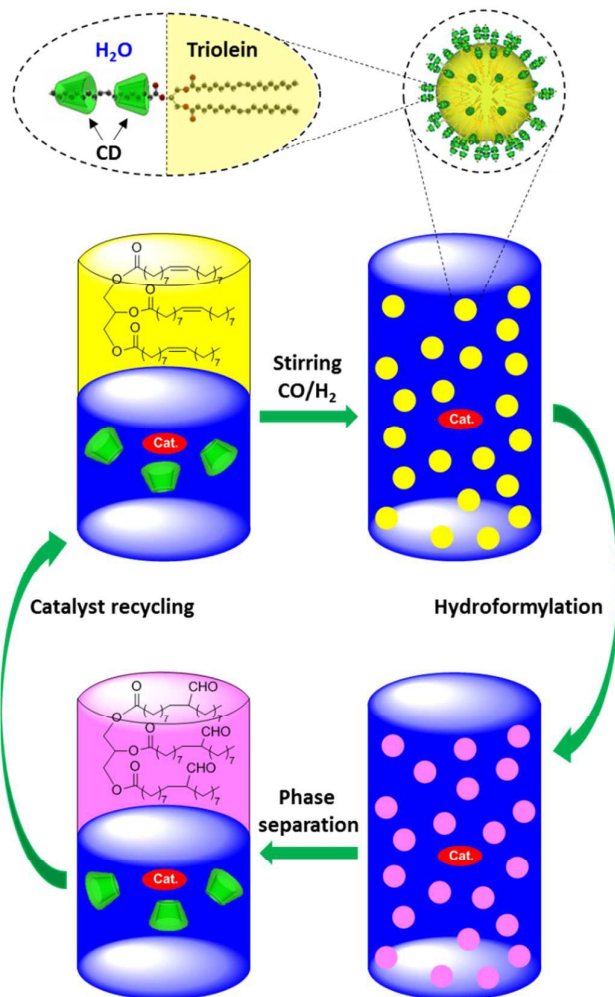


Fig. 1 Concept of the self-emulsifying catalytic system with triolein (T) as a model substrate. Cat. = rhodium catalyst. Cyclodextrins (CD) are represented in green

In line with researches aiming at investigating the Rh-catalysed hydroformylation of alkenes using water/organic solvent systems,²⁰⁻²⁹ our group developed since 2012 the hydroformylation of vegetable oils in aqueous media. Activated carbons such as Nuchar® WV-B acted as effective interfacial additives at the aqueous/organic interface to help hydroformylate unsaturated biosourced substrates under mild conditions.³⁰ High conversions

(up to 95%) and aldehyde selectivities (up to 90%) were obtained. Additionally, the catalytic system could be efficiently recycled without significant loss neither in conversion nor aldehyde selectivity. We also demonstrated that a Pickering emulsion (emulsion stabilized by solid particles) consisting of hydrophobic substrates, crystallites of α -CD/PEG (α -CD, cyclic oligomer consisting of six glucopyranose units bridged through 1,4-glycosidic bonds; PEG, poly(ethylene glycol) and a hydrogel phase allowed for a significant increase in the molecular contacts between the substrates and the Rh-catalyst dissolved in the hydrogel.³¹ Addition of randomly methylated β -cyclodextrin (RAME- β -CD, cyclic oligomer consisting of 7 glucose units bridged through 1,4-glycosidic bonds, average number of methyl groups = 12.6) in the system greatly favored the interfacial process.³²

Very recently, we implemented a new concept based on the use of modified cyclodextrins (CDs) to convert triglycerides via supramolecular means in aqueous media.^{33,34} More precisely, the alkenyl chains of triglycerides supramolecularly interacted with CDs solubilized in an aqueous phase to form in situ CD/triglyceride complexes which acted as emulsifiers in the biphasic system (Fig. 1). The amphiphilic character of the CD/triglyceride complexes allowed for the formation of a transient oil-in-water (O/W) emulsion. The enhanced interface between the catalyst-containing aqueous phase and the substrate-containing organic phase resulted in an increase in the molecular contacts between the triglyceride C=C double bonds and the water soluble Rh-catalyst, leading to a substantial increase in the conversion and selectivity of the hydroformylation reaction. Because of the weak interaction between the hydroformylated product (aldehyde) and the CD cavity, a rapid decantation took place at the end of the reaction which allowed for an easy recovery of the hydroformylated products in one phase and the water soluble Rh-catalyst in the other. The catalytic system could even be efficiently recycled using the recovered catalytic aqueous phase. Once the proof-of-concept was validated, we performed an extended study on the use of supramolecular self-emulsifiers in the Rh-catalysed hydroformylation of triglycerides.

Herein, we reported all the aspects of the study through a detailed characterization of the CD/triglycerides complexes and their catalytic performance. We especially explained how the CD and the nature of its substituents were determining in the formation of the transient O/W emulsion within which the contacts between the triglyceride and the water soluble Rh-catalyst were favoured.

Results and discussion

Phase diagrams

Triolein (T, Fig. 1) was chosen as a model substrate. Compared to technical grade triglycerides, its purity and symmetrical structure derived from glycerol and oleic acid has the significant advantage of facilitating the analysis of the reaction products. Concurrently, CDs of industrial relevance were chosen. Besides the native α -, β - and γ -CDs, we considered modified CDs such as methylated (RAME) and hydroxypropylated (HP) α -, β - and γ -CD and a weakly methylated β -CD (CRYSMEB) (Table 1). Ternary phase diagrams were constructed for CD/T/water mixtures. The three components were shaken vigorously and the mixture was allowed to stand for a given time. The resulting phase was then reported on the phase diagram. Varying the temperature, the resting time (after shaking)

and the relative proportions of CD, **T** and water allowed determining different areas on the graph.

Table 1 Description of modified CDs used in the present study.

CD	Substituent (R)	Carbons bearing R	Average number of R per CD
RAME- α -CD	-CH ₃	2, 3 and 6	10.8
RAME- β -CD	-CH ₃	2, 3 and 6	12.6
RAME- γ -CD	-CH ₃	2, 3 and 6	14.4
HP- α -CD	-CH ₂ -CHOH-CH ₃	2, 3 and 6	4.8
HP- β -CD	-CH ₂ -CHOH-CH ₃	2, 3 and 6	5.6
HP- γ -CD	-CH ₂ -CHOH-CH ₃	2, 3 and 6	6.4
CRYSMEB	-CH ₃	2, 3 and 6	4.9

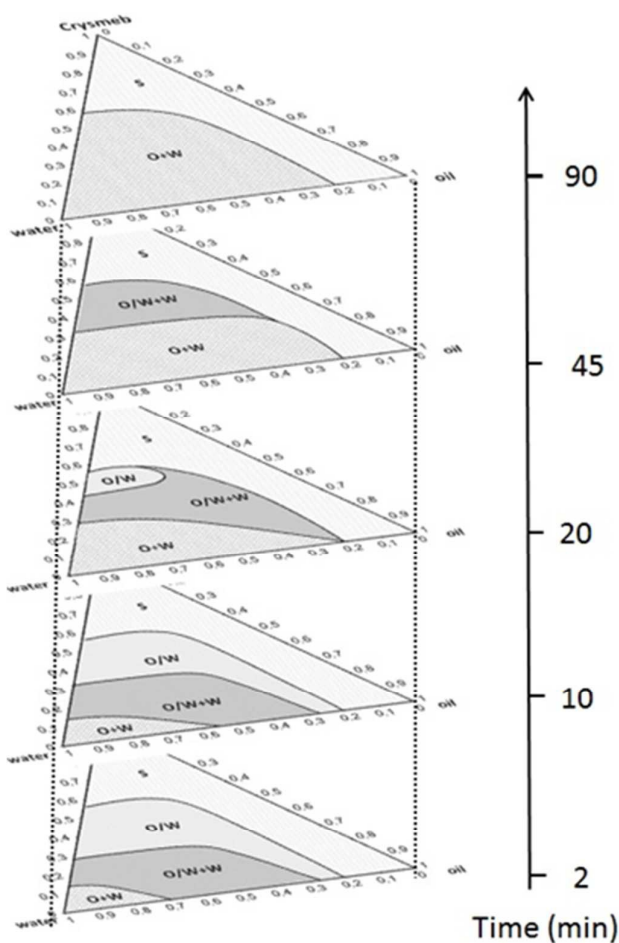


Fig. 2 Phase diagrams of CRYSMEB at room temperature as a function of the resting time after shaking.

Whatever the concentration in native α - or β -CDs, three areas could be defined on the graphs: **O+W** = a stable two-liquid-phase; **O/W+W** = an oil-in-water + water phase (turbid mixture); **S** = a solid containing phase (see Supporting Information). The relative stability of the **O/W+W** phase prevented any decantation on a reasonable time (<1h). The use of native CDs thus proved to be inappropriate for catalytic applications. Conversely, four different areas could be observed for mixtures containing RAME- β -CD, HP- β -CD or CRYSMEB (Fig. 2): **O+W** = a stable two-liquid-phase region; **O/W+W** = an unstable oil-in-water + water phase; **O/W** = an unstable oil-in-water emulsion; and **S** = a solid-containing phase. The instability of the **O/W+W** and **O/W** phases showed that modified CDs were appropriate to favor contacts between **T** and the aqueous phase without formation of stable emulsions. The extent of the four areas appeared to be dependent upon the resting time after which the observation was made once the CD, **T** and water were shaken together. Thus, a ternary phase diagram realized with data obtained after shaking and 2 min rest appeared to be very different from a ternary phase diagram obtained with data collected after shaking and 90 min rest (Fig. 2). The explanation lies in the instability of the **O/W+W** and the **O/W** phases. Indeed, both **O/W+W** and **O/W** ended up disappearing resulting in an area whose extent decreased with time.

Moreover, the extent of the phase diagrams also depended upon the temperature. As an example, the phase diagrams constructed with CRYSMEB/**T**/water and RAME- β -CD/**T**/water mixtures shaken and allowed to stand for 2 min at room temperature, 50 °C and 80 °C revealed an increase in the area of the **O+W** phase and a decrease in the area of the **O/W** phase (Fig. 3 and 4). The CD methylation degree also affected the extent of the other phases. For example, more extended area were observed for the **O/W+W** phase of a CRYSMEB/**T**/water mixture when compared to a RAME- β -CD/**T**/water mixture.

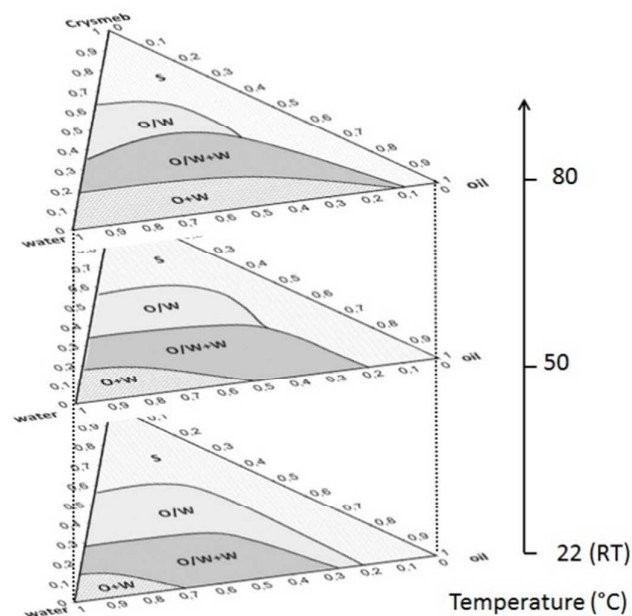


Fig. 3 Phase diagrams of CRYSMEB as a function of the temperature (resting time = 2 min).

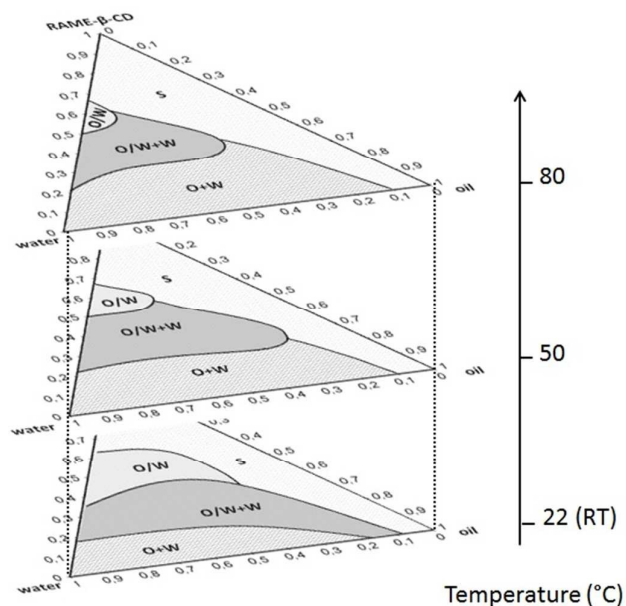


Fig. 4 Phase diagrams of RAMEB as a function of the temperature (resting time = 2 min).

Nephelometric measurements of the emulsions stability

The presence of numerous small droplets in the emulsion greatly affects the passage of light through the solution. Optical measurements are therefore a powerful tool to study the stability of the emulsion. The general principle relies on the study of the transmission (turbidimetry) or the backscattering (BS) (nephelometry) of a light beam through the emulsion. Fig. 5 showed that nephelometric measurements realized using a RAME-β-CD based emulsion confirmed the above results.

Immediately after shaking, the BS of the emulsion was constant along the vessel because of the apparent homogeneity of the emulsion. Quickly, the BS at the bottom of the vessel clearly decreased while an increase of the BS was measured at the top of the vessel. The results indicated that the droplets stabilized in the aqueous solution during the shaking phase tended to go back up to the surface where they finally coalesced. The decantation rate, measured from the variation of the clarification front at different times, were 0.37, 0.89 and 1.37 mm.min⁻¹ for RAME-CDs, HP-CDs and CRYSMEB, respectively (5%wt CD, 85%wt water and 10%wt triolein). From the decantation rate, we used the Stokes equations to calculate the hydrodynamic radius of the droplets in the emulsions (ESI). For example, they turned to be 17.8, 27.6 and 33.8 μm for RAME-β-CDs, HP-β-CDs and CRYSMEB, respectively. As expected, the wider the droplets, the faster the decantation.

Stoichiometry of the cyclodextrin/triolein complexes

The formation of such emulsions is a consequence of the existence of CD/T supramolecular complexes at the aqueous/organic interface. Their presence was clearly established by surface tension measurements.

From the variations of the surface tension γ at the T/water interface and the Gibbs equations, both the interfacial excess and interfacial area were determined for each CD/T couple (Supporting Information). The CD/T stoichiometries were determined from these data and were found to be 2.5, 1.19 and 0.95 for RAME-α-CD,

RAME-β-CD and RAME-γ-CD, respectively. These results clearly showed the high affinity of T for RAME-α-CD and the low interaction existing between RAME-γ-CD and T. These values were in line to those found for HP-β-CD and CRYSMEB (1.5/1 and 2/1, respectively).³³

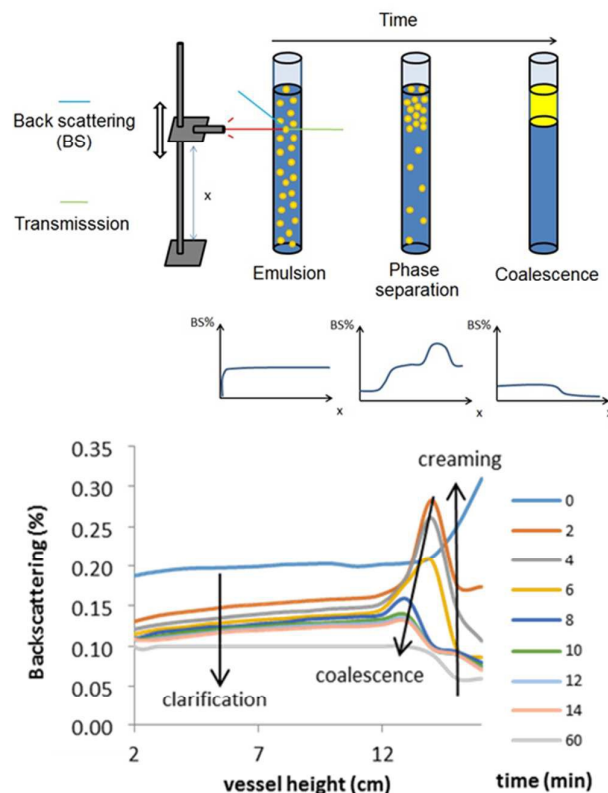


Fig. 5 Nephelometric measurements with time (in min) of a RAME-β-CD emulsion (CD: 5%wt, water 80%wt, T 15%wt).

Molecular dynamics simulation

The existence of CRYSMEB/T inclusion complexes and aggregates derived therefrom was confirmed by a molecular dynamics simulation that described the arrangement of the CRYSMEB/T supramolecular complexes at the aqueous/organic interface. Considering the difficulty of simulating the spontaneous formation of a large micelle from a random distribution of monomers, as a preliminary step, we built a biphasic systems from cubic boxes with sides of 50 Å containing 567 hexane and 4166 water molecules into which the solute (CRYSMEB/T) was immersed (Fig. 6). Cluster analysis of the MD simulation provided us a series of stable structures, the most stable one (Fig. 7) was used to preconstruct aggregate of CRYSMEB/T immersed in water. Thereafter, a 50 ns MD simulation was realized, the final obtained structure is depicted in Fig. 8. The MD simulation confirmed the existence of CRYSMEB/T aggregates in water and clearly exclude the dislocation of this molecular object into discrete CRYSMEB/T entities.

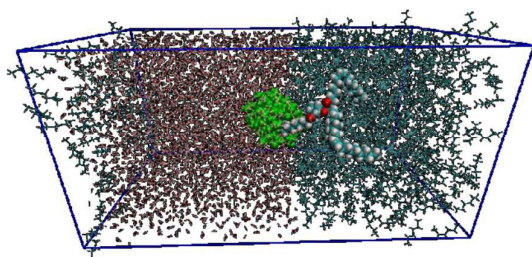


Fig. 6 Simulation box containing one CRYSMEB/T complex immersed in a water/hexane biphasic system.

Conditions of the hydroformylation reaction

Once the phase diagrams were constructed for each CD, we were able to determine the appropriate conditions for the Rh-catalyzed hydroformylation of higher olefins. The concentrations in CD, **T** and water were chosen in the largest unstable **O/W+W** region. This choice was guided by both the necessity to avoid solid particles in the catalytic system and to favour the existence in the solution of a large surface area between the substrate-containing phase and the catalyst-containing phase, especially at 80 °C (temperature at which the hydroformylation reaction took place). $[\text{Rh}(\text{CO})_2(\text{acac})]$ (acac = acetylacetonate) was chosen as a rhodium precursor and the sodium salt of the trisulfonated triphenylphosphane (TPPTS) as a water-soluble ligand to retain the Rh-catalyst in the aqueous compartment. Once dissolved in water in the presence of CD, the resulting aqueous solution was cannulated into an autoclave beforehand purged with nitrogen. **T** was then introduced through cannula and the autoclave was heated to 80 °C and pressurized under 80 bar CO/H_2 (1/1). After reaction, the autoclave was cooled down to room temperature and depressurized.

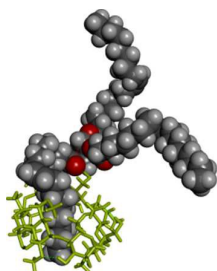


Fig. 7 CRYSMEB/T stable structure obtained from cluster analysis of all the configurations sampled throughout the trajectories at 300 K.

The absence of interaction between the aldehydes and the CD cavity led to a rapid decantation of the product-containing organic phase and the catalyst-containing aqueous phase.³³ Once the decantation of the biphasic system was complete, the organic phase was analyzed by NMR. Several series of experiments were carried out to determine the limits of the catalytic system.

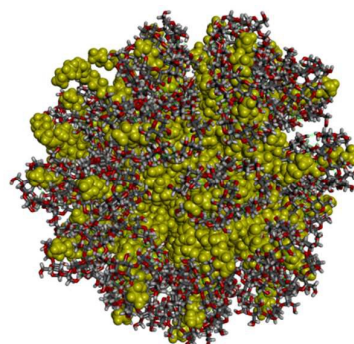


Fig. 8 Final supramolecular arrangement of CRYSMEB/T complexes after 50 ns. The **T** molecules are distinguished by yellow color. Water molecules are not shown for clarity.

Table 2 Rh-catalyzed hydroformylation of **T** with respect to the nature of the CD and its mass concentration.^a

Entry	CD	conc. (mol.L ⁻¹)	Conv.(%) ^b	Aldehyde sel.(%) ^b
1	RAME-β-CD	0.13	9	57
2	RAME-β-CD	0.26	29	83
3	RAME-β-CD	0.52	53	86
4	RAME-β-CD	0.67	52	81
5	HP-β-CD	0.06	23	70
6	HP-β-CD	0.12	43	84
7	HP-β-CD	0.46	91	90
8	HP-β-CD	0.69	87	89
9	CRYSMEB ^c	0.06	61	85
10	CRYSMEB ^c	0.12	79	97
11	CRYSMEB ^c	0.22	96	94
12	CRYSMEB ^c	0.31	94	94 ^d
13	RAME-α-CD	0.50	38	83
14	RAME-γ-CD	0.50	32	87
15	HP-α-CD	0.52	29	81
16	HP-γ-CD	0.52	87	90
17 ^e	CRYSMEB	0.22	88	94
18 ^{e,f}	CRYSMEB	0.22	90	93

^a Conditions: **T** (1 mL, 1 mmol), $\text{Rh}(\text{CO})_2(\text{acac})$ (3.9 mg, 0.015 mmol), TPPTS (mg, 0.075 mmol), water (8.2 mL), 18 h, 80 °C, 80 bar CO/H_2 (1/1).

^b determined by NMR. ^c 6 h. ^d no decantation once the reaction was complete. ^e 4 h. ^f with freshly prepared $\text{HRh}(\text{CO})(\text{TPPTS})_3$ (28 mg, 0.015 mmol) as a rhodium precursor.

Effect of the CD in the hydroformylation reaction

The nature of the CD was varied to assess the effect of its mass concentration, its size, its substituents and the substitution degree on the catalytic performance (Table 2). The best results were obtained at 80 °C under 80 bar CO/H₂ using CRYSMEB (Table 2, entry 11) and to a less extent HP-β-CD (Table 2, entry 7) and HP-γ-CD (Table 2, entry 16). Under the same catalytic conditions, RAME-CDs and α-CDs proved to be less effective. Accordingly, the nature of the substituents, the CD substitution degree and the size of the CD cavity appeared to be key parameters to control the catalytic activity and selectivity. However, it seems inappropriate at this stage to rationalize the impact of the CD structure on its recognition ability toward the **T** alkenyl chains under catalytic conditions (see for example Table 2, entries 14 and 16). No significant difference was observed using Rh(CO)₂(acac) or freshly prepared HRh(CO)(TPPTS)₃ as rhodium precursors (compare entries 17 and 18 in Table 2).

Effect of the reaction temperature

Changing the reaction temperature dramatically affected the catalytic performance (Table 3). The best conversions and aldehyde selectivities were obtained at 80 °C regardless the nature of the CD (Table 3, entries 3, 9 and 14). Note that an optimal conversion was also obtained with CRYSMEB at 60 °C. However, the aldehyde selectivity was slightly lower in that case. A temperature of 80 °C was the best compromise to finely disperse the organic phase in the aqueous solution. The contacts between the triglycerides and the Rh-catalyst being favored, the conversions were improved. Above 80 °C, the conversion was significantly affected. For example, the conversion was divided by a factor of six using HP-β-CD at 80 °C and 120 °C (compare Table 3, entries 9 and 11).

A similar trend was observed for the aldehyde selectivity. Accordingly, contrary to what was usually observed,³⁵ increasing the reaction temperature did not improve the catalytic performances. These results are in line with the above phase diagrams and the observations made by optical microscopy.³³ Logically, upon increasing the temperature, the area of the **O/W+W** phase is significantly reduced on the phase diagram and the chosen catalytic conditions are then outside this area.

Effect of the CO/H₂ pressure

Variations of the CO/H₂ pressure significantly impacted the conversion and the aldehyde selectivity. A CO/H₂ pressure of 20 bar was clearly insufficient and revealed the limitation in the syngas diffusion throughout the biphasic system (Table 4, Entry 1). Increase of the CO/H₂ pressure to 50 bar gave better but not optimal results (Table 4, Entry 2). Conversely, very good conversions and aldehyde selectivities were obtained for CO/H₂ pressure above 80 bar. These results were in line with previous results obtained on linear terminal alkenes.³⁶ Note that increasing the CO/H₂ pressure to 100 bar did not affect the catalytic results. However, a variation of the CO/H₂ ratio significantly alter the conversion and/or the selectivity. Increasing the CO pressure with respect to the H₂ pressure led to a decrease in both the conversion and the aldehyde selectivity (Table 4, Entry 5). Indeed, the displacement of the equilibriums toward CO-rich Rh-species disfavored the insertion of the C=C double bonds. On the contrary, hydrogen-rich mixture of CO/H₂ led to a higher proportion of hydrogenated side-products (table 4, Entry 6).

Table 3 Effect of the reaction temperature in the Rh-catalyzed hydroformylation of **T**.^a

Entry	CD	Temp. (°C)	Conv.(%) ^b	Aldehyde sel.(%) ^b
1	RAME-β-CD ^b	40	36	78
2	RAME-β-CD ^b	60	45	86
3	RAME-β-CD ^b	80	53	85
4	RAME-β-CD ^b	100	34	48
5	RAME-β-CD ^b	120	23	28
6	HP-β-CD ^b	30	28	68
7	HP-β-CD ^b	50	50	79
8	HP-β-CD ^b	60	60	82
9	HP-β-CD ^b	80	78	85
10	HP-β-CD ^b	100	48	65
11	HP-β-CD ^b	120	13	23
12	CRYSMEB ^c	40	69	87
13	CRYSMEB ^c	60	96	88
14	CRYSMEB ^c	80	96	94
15	CRYSMEB ^c	100	74	84
16	CRYSMEB ^c	120	36	70

^a Conditions: **T** (1 mL, 1 mmol), Rh(CO)₂(acac) (3.9 mg, 0.015 mmol), TPPTS (42 mg, 0.075 mmol), water (8 mL), 80 bar CO/H₂ (1/1), 18 h. ^b determined by NMR. ^c 0.52 mol.L⁻¹. ^d 0.20 mol.L⁻¹.

Table 4 Effect of the CO/H₂ pressure in the Rh-catalyzed hydroformylation of **T**.^a

Entry	CO/H ₂ pressure (bar)	Conv.(%) ^(b)	Aldehyde sel.(%) ^(b)
1	20 (1/1)	18	55
2	50 (1/1)	69	83
3	80 (1/1)	96	94
4	100 (1/1)	96	92
5	80 (2/1)	85	86
6	80 (1/2)	96	74

^a Conditions: **T** (1 mL, 1 mmol), Rh(CO)₂(acac) (3.9 mg, 0.015 mmol), CRYSMEB (2 mmol), TPPTS (42 mg, 0.075 mmol), water (8 mL), 80 °C, 6 h. ^b determined by NMR.

Effect of the water soluble phosphane

Various water soluble phosphanes were compared to TPPTS (Figure). The catalytic results were summarized in Table 5. No significant difference could be noticed between TPPTS and its *para*-methyl and *para*-methoxy derivatives (Table 5, entries 2 and 3), meaning that the *para*-substitution on the phenyl groups of the phosphane did not affect the catalytic performance. Conversely, *ortho*-substituted ligands led to better conversions (Table 5, entries 4 and 5). However, the aldehydes selectivities were lower. Moreover, the experiments carried out with *ortho*-substituted phosphanes showed a lixiviation of the Rh-catalyst to the organic phase. This was a consequence of the steric hindrance generated around the metal center by the bulky *ortho*-substituted phosphane. Phosphane low-coordinated rhodium species were then formed during the course of the reaction. The catalyst being less coordinated by water soluble phosphanes, it was then transferred to the organic phase where it reacted directly with the C=C double bonds under homogeneous conditions.

Table 5 Effect of the phosphane in the Rh-catalyzed hydroformylation of T.^a

Entry	Phosphane	Conv.(%) ^b	Aldehyde Sel.(%) ^b	Leaching
1	TPPTS	53	86	no
2	Tris(pMe)TPPTS	53	83	no
3	Tris(pOMe)TPPTS	50	86	no
4	Tris(oMe) TPPTS	81	75	yes
5	Tris(oOMe)TPPTS	83	80	yes
6	Tris(pCl)TPPDS	82	82	yes
7	BDPPTS	58	85	no
8	DBPPTS	52	86	no
9	TBPTS	51	82	no
10	BPPBTS	2	nd	no
11	SulfoXantphos	0	nd	no

^a Conditions: T (1 mL, 1 mmol), RAME-β-CD (2 mmol), Rh(CO)₂(acac) (3.9 mg, 0.015 mmol), water (8 mL), 80 °C, 80 bar CO/H₂ (1/1), 18 h.

^b determined by NMR.

The less coordinated rhodium species was very active but less selective. Consequently, the aldehyde selectivity strongly decreased to the profit of the C=C hydrogenation. The use of Tris(pCl)TPPDS allowed for a significant increase in the C=C conversion with aldehyde selectivity up to 82% (Table 5, entry 6). However, the catalytic performance probably resulted from the high surface

activity of this disulfonated phosphane. Once the reaction was complete, the aqueous phase was colorless and black particles could be observed at the interface, suggesting that the Rh-catalyst was not stable under these conditions. Phosphanes substituted by biphenyl groups were also tested as our group previously showed that such phosphanes could form second sphere ligands (by interaction with the CD cavity) capable of modifying the catalytic activity and selectivity.^{37,38} However, no significant variations in the catalytic performance was noticed (Table 5, entries 7, 8 and 9). Thus, even though second sphere ligands were formed during the course of the reaction, their impact on the catalytic system were negligible. Bidentate ligands were clearly inappropriate for this self-emulsified biphasic system as conversions were very low (Table 5, entries 10 and 11). Generally, bidentate ligands required higher reaction temperatures.²⁴ However, the studied emulsions would not tolerate higher temperatures as they would be destabilized.

Effect of the rhodium precursor

Various metallic precursors were assessed and compared to Rh(CO)₂(acac) (Table 6).

Table 6 Effect of the rhodium precursor in the Rh-catalyzed hydroformylation of T.^a

Entry	Metallic precursor	Conv.(%) ^b	Aldehyde sel.(%) ^b
1	Rh(CO) ₂ (acac)	53	86
2	Rh(COD) ₂ BF ₄	53	81
3	RhCl ₃	19	60
4	[Rh(COD)Cl] ₂	23	62
5	Co ₂ (CO) ₈	<1	nd

^a Conditions: T (1 mL, 1 mmol), CRYSMEB (2 mmol), metallic precursor (0.015 mmol), TPPTS (42 mg, 0.075 mmol), water (8 mL), 80 °C, 80 bar CO/H₂ (1:1), 18 h. ^b determined by NMR.

Rh(CO)₂(acac) was clearly the best metallic precursor both in terms of conversion and aldehyde selectivity (Table 6, entry 1). Similar results were obtained using Rh(COD)₂BF₄ as a precursor (albeit the aldehyde selectivity was a little bit lower) (Table 6, entry 2). Conversely, low conversions were obtained using RhCl₃ and [Rh(COD)Cl]₂ probably because of the formation of HCl during the course of the reaction (Table 6, entries 3 and 4). The presence of a strong acid such as HCl in the medium prevented the formation of the Rh-hydride species.³⁹ The cobalt precursor also proved to be ineffective (Table 6, entry 5). Indeed, harsher experimental conditions were required for the hydroformylation to proceed using cobalt precursors.⁴⁰ However, the studied self-emulsifying system imposed mild conditions, especially a reaction temperature around 80 °C.

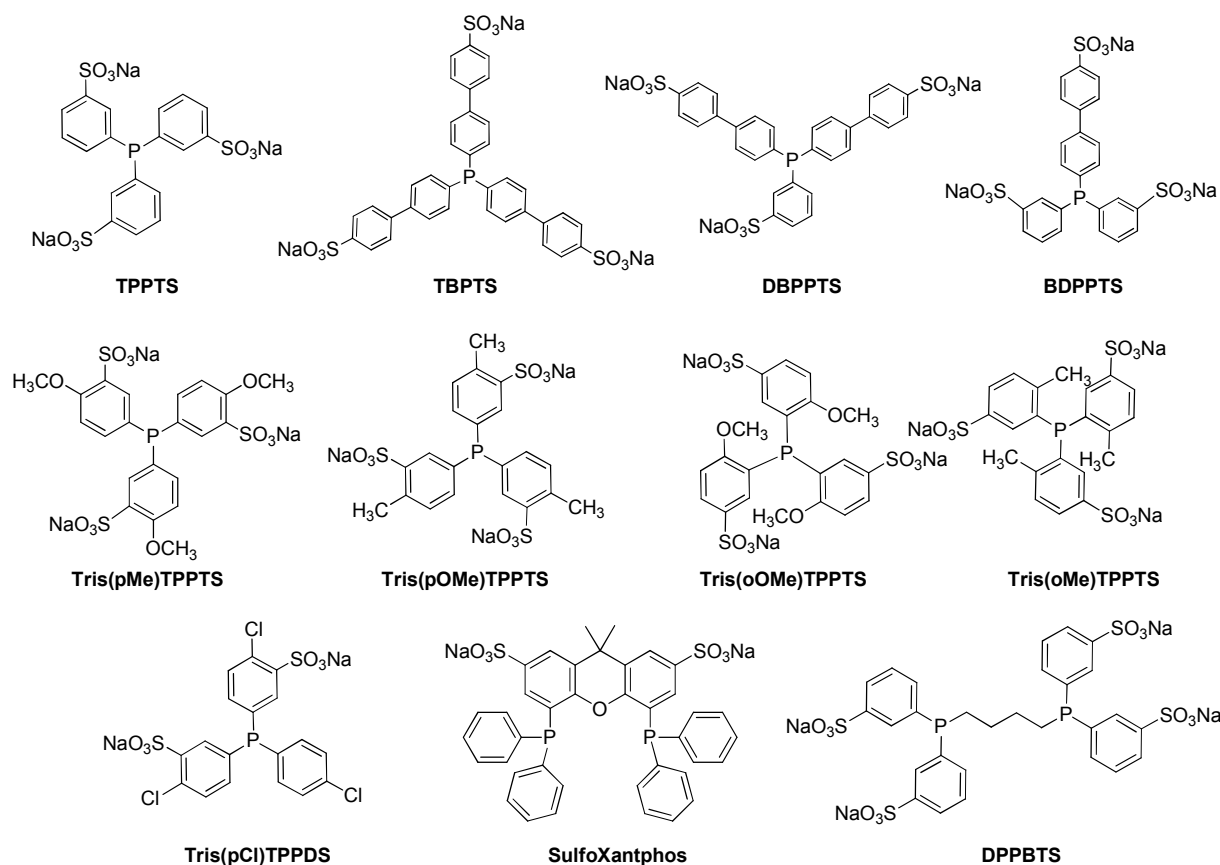


Fig. 9 Studied water-soluble phosphanes.

Table 7 Rh-catalyzed hydroformylation of commercial oils.^a

Entry	CD	Oil	Avg. No. C=C ^c	Conv. (%) ^b	Ald. sel. (%) ^b	Conj. Sel. (%) ^b
1	RAME-β-CD	Olive	2.78	48	71	-
2	RAME-β-CD	Sesame	3.75	37	16	60
3	RAME-β-CD	Soy	4.36	39	3	73
4	HP-β-CD	Olive	2.78	78	85	-
5	HP-β-CD	Sunflower	2.75	51	80	6
6	HP-β-CD	Sesame	3.75	33	4	74
7	HP-β-CD	Rapeseed	3.69	38	35	27
8	CRYSMEB	Olive	2.78	86	86	-
9	CRYSMEB	Sunflower	2.75	54	80	7
10	CRYSMEB	Sesame	3.75	34	20	66

^a Conditions: T (1 mL, 1 mmol), Rh(CO)₂(acac) (3.9 mg, 0.015 mmol), TPPTS (42 mg, 0.075 mmol), water (8 mL), 80 bar CO/H₂ (1/1), 18 h. ^b determined by NMR and GC. ^c Avg. No. C=C: average number of C=C per chain for each oil.

Hydroformylation of commercial oils

Once the experimental conditions were optimized, the scope of the catalytic system was broadened to commercial oils. Unlike **T** that has only one unsaturated fatty chain and whose purity of the commercial sample used in this study is high (> 97%), most of the triglycerides from vegetable origin have a variable fatty acid composition and a variable number of unsaturations per chain. These fatty chains are most generally a statistical mixture of mono- or polyunsaturated C18 fatty acids. In Table 7 are given the average number of C=C double bond per chain for each oil. Contrary to **T**, the hydroformylation of polyunsaturated triglycerides revealed an isomerization reaction of the double bonds. It is however known from the literature that rhodium catalysts allow for the isomerization of polyunsaturated compounds to their conjugated forms.^{41,42,43,44} There seemed to be a correlation between the conversions and the proportion of conjugated fatty chains formed during the reaction. Indeed, for oils with a high proportion of polyunsaturated chains (linoleic and linolenic chains) such as soy and sesame oils, the organic phase was strongly colored once the reaction was complete, indicative of a catalyst leaching (Table 7, entries 3, 6 and 10). Moreover, the overall conversion decreased and the aldehyde selectivity declined in favor of the isomerization of the double bonds. The explanation lies in the coordinating ability of conjugated dienes that trapped rhodium in the organic phase as a π -allyl complex, thus preventing subsequent conversion of the C=C double bonds.^{45,46}

Conclusions

In summary, we found that the C=C double bonds of triglycerides can be readily converted into aldehydes using an aqueous biphasic system for which an organometallic Rh-complex is retained within the aqueous compartment. The triglycerides drive their own conversion because of the substantial decrease in the surface tension resulting from the formation of transient CD/triglyceride supramolecular complexes at the aqueous/organic interface. Through a detailed study on the additives and catalytic parameters, we showed that weakly substituted CDs such as CRYSMEB especially proved to be very effective in this context. Interestingly, the studied catalytic system could be efficiently applied to the hydroformylation of commercial oils, especially those with a low average number of carbon-carbon double bonds. Through supramolecular means, we are currently developing other catalytic reactions using this novel biphasic system. Indeed, there appears considerable scope for using transient CD/guest supramolecular complexes to promote both catalytic activity and selectivity in organometallic reactions. More generally speaking, these host/guest complexes could become a popular tool in the hands of chemists interested in supramolecular interactions. It is likely that this new supramolecular approach will have repercussions in other fields than catalysis, as far as a dynamic interface is concerned.

Experimental

(a) Hydroformylation reactions

General procedure: In a typical experiment, $\text{Rh}(\text{CO})_2(\text{acac})$ (39 mg, 0.015 mmol, 1 eq) TPPTS (42 mg, 0.075 mmol, 5 eq) and CRYSMEB (2.3 g, 2 mmol) were degassed by vacuum- N_2 cycles three times and were dissolved in degassed deionized water (3.4 mL). The resting solution was stirred at room temperature until all the rhodium complex was dissolved (4 h). 1 mL of triolein (0.91 g, 1 mmol) was poured into the autoclave and N_2 -purged. The catalytic solution was then cannulated under nitrogen into the autoclave. Once a temperature of 80 °C has been reached, the autoclave was pressurized under CO/H_2 pressure (80 bar) and the solution was vigorously stirred (1500 rpm). When the reaction was over, the apparatus was allowed to cool to room temperature and depressurized. The organic phase was extracted directly after opening the autoclave thank to products decantation. The products were analyzed by ^1H and ^{13}C NMR experiments. All runs have been performed at least twice in order to ensure reproducibility.

(b) Molecular dynamics simulation

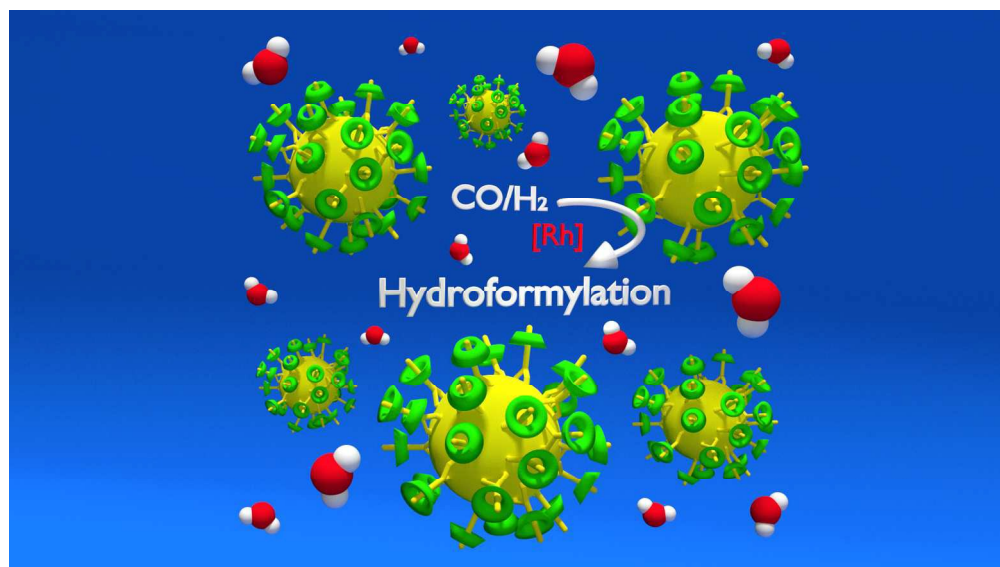
For the whole simulation procedure the Amber10 suite of program⁴⁷ was used with the general force field parameters (GAFF)⁴⁸ and TIP3P water model.⁴⁹ Atomic charges for the solute molecules were obtained by the restrained electrostatic potential (RESP) methodology, electrostatic potentials were generated at DFT (B3LYP) level with 631G* basis set. The DFT calculations were performed with Gaussian03 software.⁵⁰ Nonbonded interactions were calculated using a 12 Å atom-based cutoff, correcting the long-range electrostatics by using the Ewald summation method (particle mesh Ewald approximation).⁵¹ The productive step was performed with 2fs time step, at 300 K and a constant pressure of 1.0 bar with isotropic position scaling. Constant temperature and pressure conditions in the simulations were achieved by coupling the system to a Berendsen's thermostat and barostat.⁵² Bonds involving the hydrogen atoms were constrained to their equilibrium position with the SHAKE algorithm.⁵³ The simulation time was 50 ns and trajectories were saved every 3 ps. This time scale is sufficient to observe an eventual spontaneous dissociation of unstable complexes.⁵⁴

Acknowledgements

This work was performed in partnership with the SAS PIVERT, within the frame of the French Institute for the Energy Transition (Institut pour la Transition Énergétique (ITE) P.I.V.E.R.T. (www.institut-pivert.com) selected as an Investment for the Future ("Investissements d'Avenir"). This work was supported, as part of the Investments for the Future, by the French Government under the reference ANR-001-01. Roquette Frères (Lestrem, France) is gratefully acknowledged for generous gifts of cyclodextrins. We thank Dr. Nicolas Kania, D. Prevost and G. Crowyn for technical assistance.

Notes and reference

- ¹ Y. Xia and R. C. Larock, *Green Chem.*, 2010, **12**, 1893–1909.
- ² J. O. Metzger, *Eur. J. Lipid Sci. Technol.*, 2009, **111**, 865–876.
- ³ J. C. Ronda, G. Lligadas, M. Galiaà and V. Cádiz, *Eur. J. Lipid Sci. Technol.*, 2011, **113**, 46–58.
- ⁴ R. Lai, M. Naudet and E. Ucciani, *Rev. Fr. Corps Gras*, 1966, **13**, 737–745.
- ⁵ R. Lai, M. Naudet and E. Ucciani, *Rev. Fr. Corps Gras*, 1968, **15**, 15–21.
- ⁶ E. H. Pryde, *J. Am. Oil Chem. Soc.*, 1984, **61**, 419–424 and references therein.
- ⁷ B. Fell, D. Leckel and Ch. Schobben, *Fat Sci. Technol.*, 1995, **97**, 219–228.
- ⁸ K. F. Muilwijk, P. C. J. Kamer and P. W. N. M. van Leeuwen, *J. Am. Oil Chem. Soc.*, 1997, **74**, 223–228.
- ⁹ P. Kandamarachchi, A. Guo and Z. Petrovic, *J. Mol. Catal. A: Chem.*, 2002, **184**, 65–71.
- ¹⁰ P. Kandamarachchi, A. Guo, D. Demydov, Z. Petrovic, *J. Am. Oil Chem. Soc.*, 2002, **79**, 1221–1225.
- ¹¹ A. N. F. Mendes, R. G. da Rosa and J. R. Gregório, *Catal. Commun.*, 2005, **6**, 379–384.
- ¹² A. N. F. Mendes, J. R. Gregório and R. G. da Rosa, *J. Braz. Chem. Soc.*, 2005, **16**, 1124–1129.
- ¹³ J. R. Gregório, R. G. da Rosa, A. N. F. Mendes and J. C. Bayón, *Catal. Lett.* **2011**, **141**, 977–981.
- ¹⁴ H. F. Ramalho, K. M. C. di Ferreira, P. M. A. Machado, R. S. Oliveira, L. P. Silva, M. J. Prauchner and P. A. Z. Suarez, *Ind. Crops Prod.*, 2014, **52**, 211–218.
- ¹⁵ A. Behr, D. Obst and A. Westfechtel, *Eur. J. Lipid Sci. Technol.*, 2005, **107**, 213–219.
- ¹⁶ E. Benetskiy, S. Luhr, M. Vilches-Herrera, D. Selent, H. Jiao, L. Domke, K. Dyballa, R. Franke and A. Börner, *ACS Catal.*, 2014, **4**, 2130–2136.
- ¹⁷ Y. Yuki, K. Takahashi, Y. Tanaka and K. Nozaki, *J. Am. Chem. Soc.*, 2013, **135**, 17393–17400.
- ¹⁸ L. Damas, G. N. Costa, J. C. Ruas, R. M. B. Carrilho, A. R. Abreu, G. Aquino, M. J. F. Calvete, M. Pineiro and M. M. Pereira, *Curr. Microwave Chem.*, 2015, **2**, 53–60.
- ¹⁹ S. Pandey, S. H. Chikkali, *ChemCatChem*, DOI: 10.1002/cctc.201500743.
- ²⁰ L. Obrecht, P. C. J. Kamer and W. Laan, *Catal. Sci. Technol.*, 2013, **3**, 541–551.
- ²¹ H. Nowothnick, A. Rost, T. Hamerla, R. Schomäcker, C. Müller and D. Vogt, *Catal. Sci. Technol.*, 2013, **3**, 600–605.
- ²² S. K. Sharma, R. V. Jasra, *Catal. Today*, 2015, **247**, 70–81.
- ²³ A. F. Cardozo, C. Julcour, L. Barthe, J.-F. Blanco, S. Chen, F. Gayet, E. Manoury, X. Zhang, M. Lansalot, B. Charleux, F. D'Agosto, R. Poli, H. Delmas, *J. Catal.*, 2015, **324**, 1–8.
- ²⁴ S. Siangwata, N. Baartzes, B. C. E. Makhubela, G. S. Smith, *J. Organomet. Chem.*, 2015, **796**, 26–32.
- ²⁵ M. Schwarze, T. Pogrzeba, K. Seifert, T. Hamerla and R. Schomäcker, *Catal. Today*, 2015, **247**, 55–63.
- ²⁷ T. Hamerla, A. Rost, Y. Kasaka and R. Schomäcker, *ChemCatChem*, 2013, **5**, 1854–1852.
- ²⁸ A. T. Straub, M. Otto, I. Usui, and B. Breit, *Adv. Synth. Catal.*, 2013, **355**, 2071–2075.
- ²⁹ D. Peral, D. Herrera, J. Real, T. Flor and J. C. Bayón, DOI: 10.1039/C5CY01004G.
- ³⁰ J. Boulanger, A. Ponchel, H. Bricout, F. Hapiot and E. Monflier, *Eur. J. Lipid Sci. Technol.*, 2012, **114**, 1439–1446.
- ³¹ J. Potier, S. Menuel, M.H. Chambrier, L. Burylo, J.-F. Blach, P. Woisel, E. Monflier and F. Hapiot, *ACS Catal.*, 2013, **3**, 1618–1621.
- ³² J. Potier, S. Menuel, E. Monflier and F. Hapiot, *ACS Catal.*, 2014, **4**, 2342–2346.
- ³³ T. Vanbésien, E. Monflier, F. Hapiot, *ACS Catal.*, 2015, **5**, 4288–4292.
- ³⁴ F. Hapiot, E. Monflier, T. Vanbésien, PCT-F 2014, R2014–052860; WO2015071580 (A1).
- ³⁵ L. Leclercq, F. Hapiot, S. Tilloy, K. Ramkisoensing, J. N. K. Reek, P. W. N. M. van Leeuwen and E. Monflier, *Organometallics*, 2005, **24**, 2070–2075.
- ³⁶ L. Gonsalvi, A. Guerriero, E. Monflier, F. Hapiot and M. Peruzzini, *Top. Curr. Chem.*, 2013, **342**, 1–48.
- ³⁷ L. Caron, H. Bricout, S. Tilloy, A. Ponchel, D. Landy, S. Fourmentin and E. Monflier, *Adv. Synth. Catal.*, 2004, **346**, 1449–1456.
- ³⁸ H. Bricout, E. Léonard, C. Len, D. Landy, F. Hapiot and E. Monflier, *Beilstein J. Org. Chem.*, 2012, **8**, 1479–1484.
- ³⁹ P. W. N. M van Leeuwen and C. Claver. in Rhodium catalyzed hydroformylation, Chap. 9, Kluwer Academic Publisher, 2002, pp 234–251.
- ⁴⁰ F. Hebrard and P. Kalck, *Chem. Rev.*, 2009, **109**, 4272–4282.
- ⁴¹ R. L. Quirino and R. C. Larock, *J. Am. Oil Chem. Soc.*, 2011, **89**, 1113–1124.
- ⁴² R. C. Larock, X. Dong, S. Chung, C. K. Reddy and L. E. Ehlers, *J. Am. Oil Chem. Soc.*, 2001, **78**, 447–453.
- ⁴³ S. Krompiec, R. Penczek, M. Krompiec, T. Pluta, H. Ignasiak, A. Kita, S. Michalik, M. Matlengiewicz and M. Filapek, *Curr. Org. Chem.*, 2009, **13**, 896–913.
- ⁴⁴ A. Behr, H. Witte and Z. Bayrak, *Eur. J. Lipid Sci. Technol.*, 2013, **115**, 721–728.
- ⁴⁵ K. F. Muilwijk, P. C. J. Kamer and P. W. N. M. van Leeuwen, *J. Am. Oil Chem. Soc.*, 1997, **74**, 223–228.
- ⁴⁶ G. Liu and M. Garland, *J. Organomet. Chem.*, 2000, **608**, 76–85.
- ⁴⁷ D. A. Case et al. (University of California, San Francisco., 2008).
- ⁴⁸ J. Wang, R. M. Wolf, J. W. Caldwell, P. A. Kollman, D. A. Case, *J. Comput. Chem.*, 2004, **25**, 1157–1174.
- ⁴⁹ W. L. Jorgensen, J. Chandrasekhar, J. D. Madura, R. W. Impey and M. L. Klein, *J. Chem. Phys.*, 1983, **79**, 926–935.
- ⁵⁰ M. J. Frisch, et al. (Gaussian, Inc., Pittsburgh PA, 2003).
- ⁵¹ T. Darden, D. York and L. Pedersen, *J. Chem. Phys.*, 1993, **98**, 10089–10092.
- ⁵² H. J. C. Berendsen, J. P. M. Postma, W. F. van Gunsteren, A. DiNola and J. R. Haak, *J. Chem. Phys.*, 1984, **81**, 3684–3690.
- ⁵³ J.-P. Ryckaert, G. Ciccotti and H. J. C. Berendsen, *J. Comp. Phys.*, 1977, **23**, 327–341.
- ⁵⁴ Á. Piñeiro, X. Banquy, S. Pérez-Casas, E. Tovar, A. García, A. Villa, A. Amigo, A. E. Mark and M. Costas, *J. Phys. Chem. B*, 2007, **111**, 4383–4392.



677x381mm (72 x 72 DPI)